

Very low recombination phosphorus emitters for high efficiency crystalline silicon solar cells

P Ortega, M Vetter, S Bermejo and R Alcubilla

Grupo de Micro y Nano Tecnologías (MNT), Departamento de Ingeniería Electrónica, Universitat Politècnica de Catalunya (UPC), C/Jordi Girona Salgado 1-3, 08034 Barcelona, Spain

E-mail: ortega@eel.upc.edu

Received 16 June 2008, in final form 26 September 2008

Published 7 November 2008

Online at stacks.iop.org/SST/23/125032

Abstract

This work studies low recombination phosphorus emitters on c-Si. The emitters are fabricated by diffusion from solid sources and then passivated by thermal oxide yielding sheet resistances between 15 and 280 Ω/sq . Emitter saturation current densities lie in the 2.5–110 fA cm^{-2} range, leading to implicit open-circuit voltages between 674 and 725 mV. Bulk lifetime is limited by intrinsic recombination mechanisms. Surface recombination velocities between 80 and 300 cm s^{-1} have been obtained, appearing among the lowest reported in this range of emitter sheet resistances.

1. Introduction

Low recombination emitters are especially relevant in high efficiency c-Si solar cells where high open-circuit voltages, V_{oc} , are required. To obtain high V_{oc} , reverse emitter saturation current density, J_{oe} , should be as small as possible. With this perspective and concerning emitter design two approaches are possible: (i) to use a heterostructure scheme in order to block the minority carriers, or (ii) to use a homostructure with well-passivated surface. Several examples using the former approach have been envisaged in the past, for instance a $\text{SiO}_x\text{:c-Si:SiO}_x$ heterostructure (semi-insulating polycrystalline silicon (SIPOS)) yields V_{oc} of 720 mV in a laboratory test structure [1], and more recently, industrial solar cells using a HIT (heterojunction with intrinsic thin layer) structure achieved a V_{oc} of 712 mV with photovoltaic efficiencies of 21.5% [2]. However, the record photovoltaic efficiency (24.7%) in a c-Si solar cell is based on the second strategy, although having only slightly lower V_{oc} value (706 mV) [3, 4]. To improve homojunction solar cells, it is necessary to increase V_{oc} toward the values achieved by heterojunction strategy using a better emitter passivation. New calculations for the limiting efficiency, taking into account intrinsic recombination mechanisms (Coulomb-enhanced Auger and radiative recombination mechanisms), give a maximum cell efficiency of 29% [5, 6]. To reach this

limit, it is mandatory to have total J_{oe} below 10 fA cm^{-2} including contacted and noncontacted regions.

Many works have explored different passivation schemes of phosphorus-doped emitters [7–9], being focused on obtaining low J_{oe} . Low J_{oe} is important, but simultaneously, the bulk lifetime of the substrate should be preserved. Additionally, emitter performance should not jeopardize electrical current–voltage characteristics (I – V curve) as a consequence of a high recombination in the depletion region near the junction (this phenomenon is modeled by a second diode in parallel with the ideal diode due to the diffusion current), penalizing severely fill factor and therefore solar cell efficiency. Therefore, the fabrication process should be designed trying to minimize J_{oe} , to maintain the lifetime in the bulk of the substrate as high as possible, and to keep the recombination at the space charge region to a minimum.

Taking into account these considerations, this work studies very low recombination emitters passivated by means of thermal dry SiO_2 and doped using solid diffusion sources for high-efficiency c-Si solar cell fabrication. Cell performance will be determined analyzing the whole dependence of effective carrier lifetime on average excess carrier density, Δn , using the quasi-steady-state photoconductance (QSS-PC) method [10, 11]. PC-1D program [12] will be used to calculate the emitter surface recombination velocity (SRV) at the $\text{SiO}_2\text{:Si(N}^+)\text{ interface}$.

2. Parameter extraction from lifetime measurements

In order to characterize the fabricated emitters, we have analyzed the injection level dependence of lifetime curves determined by the QSS-PC method. The measured dependence of effective lifetime with Δn takes into account bulk and emitter recombination according to

$$\begin{aligned} \frac{1}{\tau_{\text{eff}}(\Delta n)} &\approx \frac{1}{\tau_{\text{in}}(\Delta n)} + \frac{1}{\tau_{\text{emit}}(\Delta n)} \\ &= \frac{1}{\tau_{\text{in}}(\Delta n)} + \frac{1}{\tau_e(\Delta n)} + \frac{1}{\tau_{\text{dep}}(\Delta n)}. \end{aligned} \quad (1)$$

Due to the high quality of float zone material, the Shockley–Read–Hall recombination mechanism has been considered negligible, and therefore bulk recombination is determined by the intrinsic mechanisms (Auger and band-to-band), τ_{in} being its related lifetime. The dependence of τ_{in} with the average carrier excess density Δn and the bulk doping concentration N_{Bulk} has been determined by Kerr [5] including photon recycling in the band-to-band mechanism with an equivalent radiative recombination coefficient of $2 \times 10^{-15} \text{ cm}^3 \text{ s}^{-1}$. Emitter recombination losses are considered by means of the τ_{emit} lifetime. A generalized emitter recombination model has two terms: emitter bulk recombination including emitter surface recombination, τ_e , and depletion region recombination, τ_{dep} . The relationship of τ_e with Δn and N_{Bulk} is given by equation (2):

$$\frac{1}{\tau_e(\Delta n)} = \frac{2J_{\text{oe}}}{qn_i^2 W} (\Delta n + N_{\text{Bulk}}). \quad (2)$$

The second term of τ_{emit} (see equation (1)) can be expressed using equation (3) [13]:

$$\frac{1}{\tau_{\text{dep}}(\Delta n)} = \frac{2J_{\text{orec}}}{qW\Delta n} \left(\frac{\Delta n(N_{\text{Bulk}} + \Delta n)}{n_i^2} \right)^{1/n_{\text{rec}}}, \quad (3)$$

where J_{orec} and n_{rec} are the reverse saturation current density and the ideality factor respectively of the second diode that takes into account recombination losses in the depletion region (typically $n_{\text{rec}} = 2$). W is the wafer thickness, and n_i is the intrinsic concentration ($n_i = 8.65 \times 10^9 \text{ cm}^{-3}$ at $T = 25^\circ \text{C}$). Since τ_{in} and τ_e are constant at low injection levels, J_{orec} and n_{rec} can be extracted analyzing the τ_{eff} dependence on Δn in this region of the $\tau_{\text{eff}}(\Delta n)$ curve. In fact, recombination in the depletion region lowers the effective lifetime in the low injection region. On the other hand, J_{oe} can be obtained from the intermediate injection level region, where the $1/\tau_{\text{eff}} - 1/\tau_{\text{in}}$ dependence is a straight line, with the slope proportional to J_{oe} . In figure 1, as an example, the asymptotic behavior of the different terms that influence the effective lifetime measurements is shown. J_{oe} , J_{orec} and n_{rec} are extracted by fitting the τ_{eff} curve in the whole injection range from 10^{13} to 10^{17} cm^{-3} . Fitting takes into account the depletion-region-modulation (DRM) effect [14]. This artifact increases the effective lifetime due to the changes in the depletion region width that increases the measured conductivity at low injection levels.

PC-1D simulations will allow us to fit the obtained J_{oe} and to relate it to the SRV at the passivated heavily phosphorus-doped silicon surface. The default program settings for the

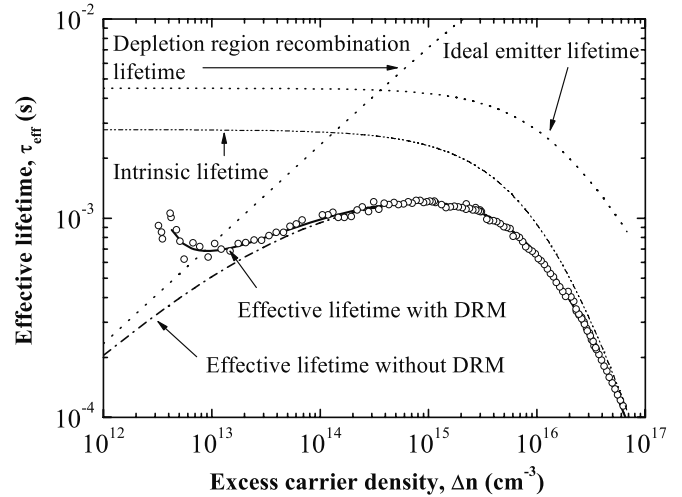


Figure 1. Measured data (symbols) and fitting (continuous line) for an annealed SiO_2 passivated emitter ($R_{\text{sh}} = 280 \Omega/\text{sq}$). Fitting takes into account all recombination mechanisms and DRM effect. Each recombination term appears separately in the graph considering its respective asymptotic behavior.

minority carrier mobility and apparent band gap narrowing have been used [8]. The minority lifetime in the emitter region has been considered Auger limited. Doping emitter profiles used in simulations have been obtained by means of a process simulator (SUPREM). To adjust measured data with simulations, especially in high doped samples, it has been necessary to reduce bulk emitter recombination considering a value of the n -type Auger coefficient, C_n , slightly lower than the default PC-1D program value (lowering from 2.2×10^{-31} to $1.2 \times 10^{-31} \text{ cm}^6 \text{ s}^{-1}$), because otherwise it overestimates bulk emitter losses. A possible explanation of this divergence between Auger values is the use in simulations of a simple model for the apparent band gap narrowing that is valid for moderate doping concentrations ($< 10^{19} \text{ cm}^{-3}$), but as already reported in the literature, fails for heavily doped emitters [9]. Therefore, a lower value of C_n possibly compensates this lack of the model.

3. Experimental results

Since we focus on solar cell applications we use p-type boron-doped substrate with resistivity $0.95 \Omega \text{ cm}$ to monitor the bulk lifetime and the recombination at the space charge region, at the same time as J_{oe} . This resistivity is compatible with the highest efficiency process. Substrates were $300 \mu\text{m}$ thick, $\langle 100 \rangle$ c-Si float zone double-side-polished $4''$ wafers. After RCA cleaning, samples were diffused simultaneously on both wafer sides at temperatures between 815 and 890°C . Next, samples were passivated with 110 nm dry thermal SiO_2 resulting in sheet resistances $R_{\text{sh}} = 15$ to $280 \Omega/\text{sq}$ of the emitters. This range covers most of the different solar cell emitter doping requirements [4, 15, 16]. Dry oxidation was performed at $T = 1060^\circ \text{C}$ for 60 min in a furnace that is routinely cleaned with dichloroethylene (DCE). The oxidations were also performed using DCE. This differs from TCA cleaning process [17] since it is a less environmentally

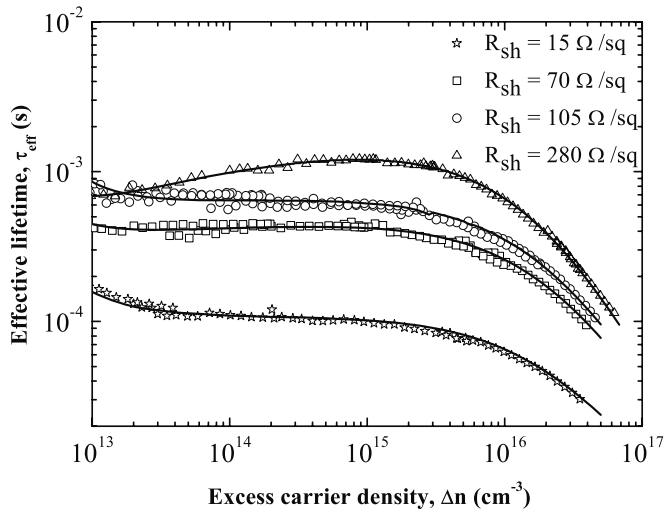


Figure 2. Lifetime measurements (symbols) and fittings (continuous lines) for FGA thermal SiO₂ passivated samples corresponding to 280, 105, 70 and 15 Ω/sq sheet resistances (both side doped samples). An annealing was performed with the 280 Ω/sq emitter.

Table 1. Parameters extracted from QSS-PC measurements and considering $n_{\text{rec}} = 2$.

R_{sh} (Ω/sq)	J_{oe} (fA cm ⁻²)	J_{orec} (nA cm ⁻²)	$J_{\text{oe}}(\text{bare})$ (fA cm ⁻²)	V_{oc} (mV) ^a	τ_{eff} (μs) ^a
280	2.5	0.70	2000	725	1000
105	11	0.40	800	716	750
70	21	0.48	600	706	580
15	110	<0.1	250	675	175

^a Extrapolated for a structure with one front side emitter and a perfect rear surface passivation (evaluated at 100 mW cm⁻² and 25 °C). An annealing was performed with the 280 Ω/sq emitter.

harmful product. After oxidation, a forming gas annealing, FGA (400 °C, 30 min), was done with all samples. In a sample of the lowest doped emitter ($R_{\text{sh}} = 280$ Ω/sq), an aluminum anneal (so-called alneal, with Al films on the oxide) was also performed [8] at 400 °C for 20 min.

QSS-PC measurements and fittings for several passivated emitters are shown in figure 2.

Table 1 summarizes parameters extracted from measurements for the four samples, where the implicit open-circuit voltage V_{oc} was calculated from QSS-PC data [18] and evaluated considering 100 mW cm⁻² solar irradiance and a temperature of 25 °C.

The thermal oxidation step after diffusion leads to very low J_{oe} values ranging from 2.5 to 110 fA cm⁻². In addition, bulk lifetime is limited by the intrinsic component to about 2.8 ms. Emitters do not have noticeable depletion region recombination, being J_{orec} below 0.5 nA cm⁻² (lower values have little impact on the electrical solar cell performance). However, the 280 Ω/sq emitter, although it has the lower J_{oe} value (2.5 fA cm⁻²), is affected by the presence of a J_{orec} term of 0.7 nA cm⁻².

Implicit V_{oc} can be extrapolated to the case of a nonsymmetrical structure with the same bulk lifetime, considering only one front side emitter, perfect passivation at the rear side, and neglecting recombination losses at the

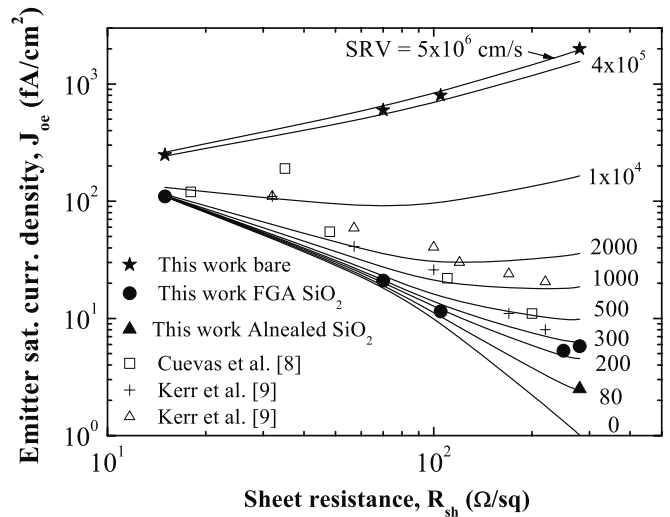


Figure 3. Comparison between our J_{oe} measurements and reported data from the literature: (□) Emitter diffusion using solid sources and passivated with thick FGA thermal oxide. (+) Emitter diffusion using POCl₃ with *in situ* drive-in and passivated with alnealed thin oxide. (Δ) Emitter diffusion using POCl₃ with *in situ* drive-in and passivated with SiN. Continuous lines show extracted J_{oe} versus R_{sh} using PC-1D program parameterized for different values of SRV.

contacts. Considering these premises, V_{oc} reaches values from 675 mV up to 725 mV (656 up to 721 mV in a symmetrical two side doped structure) with effective lifetimes between 175 and 1000 μs. It is important to remark that the maximum V_{oc} value, considering only intrinsic recombination mechanisms, is 725 mV for the resistivity and wafer thickness used in this work.

Extracted J_{oe} data of passivated and bare (after etching SiO₂) emitters are shown in figure 3 and compared with additional results extracted from the literature.

As can be seen in figure 3, J_{oe} values appear to be among the lowest values reported in phosphorus-doped emitters in the range of 15–280 Ω/sq. An excellent passivation is achieved with SRVs in the range of 80–300 cm s⁻¹ with surface doping concentrations between 4.5×10^{18} and 7.3×10^{19} cm⁻³. It is important to remark that the extraction of the SRV parameter is difficult, especially in our higher doped emitters, because bulk emitter recombination dominates and masks the surface recombination for low SRV values (<1000 cm s⁻¹). Note that samples have very low SRV values near zero in the absence of an aluminum anneal. We can conclude that the oxidation process is well designed for emitter passivation purposes and only in very low doped emitters can it be useful to perform an annealing step.

From data of table 1, it is possible to envisage the total emitter recombination of a laboratory 100 Ω/sq solar cell of 1% contacted area. In this case, J_{oe} can be estimated to be 20 fA cm⁻². Besides, if a nearly perfect rear passivation is achieved, V_{oc} can be higher than 706 mV. Using a selective emitter scheme with a doping of 15 Ω/sq below contacts (1% contact area), and 280 Ω/sq in the noncontacted regions, J_{oe} and V_{oc} yield 5 fA cm⁻² and 721 mV, respectively. In the case of 70 Ω/sq (compatible with screen printed contacts) with a 10% contacted area, these figures go to 80 fA cm⁻² and around 680 mV, respectively.

4. Conclusions

In this work, we present a study of thermal oxide passivated phosphorus emitters. The reverse saturation current density, J_{oe} , is calculated by measuring the injection level dependence of the effective lifetime using the quasi steady-state photoconductance (QSS-PC) method. J_{oe} in passivated emitters is in the range from 2.5 to 110 fA cm⁻² as the sheet resistance decreased from 280 to 15 Ω /sq. Implicit V_{oc} values (at 100 mW cm⁻² and 25 °C) ranging from 675 to 725 mV are achieved. To our knowledge, this is one of the best achieved passivations with SRVs between 80 and 300 cm s⁻¹ in all the sheet resistance range. Besides, bulk lifetime is in major part limited by the intrinsic recombination mechanisms, confirming that thermal steps (predeposition and drive-in) preserve the quality of the original substrates.

Acknowledgments

Authors wish to thank Saint-Gobain Advanced Ceramics Corp. for the delivery of Planar Diffusion Sources (PDS®). One of the authors (MV) gratefully acknowledges the support of the Program 'Ramon y Cajal' of the Spanish government. This work was funded by CICYT under program TEC2005-02716/MIC.

References

- [1] Yablanovitch E, Gmitter T, Swanson R M and Kwark Y H 1985 *Appl. Phys. Lett.* **47** 1211
- [2] Taguchi M, Sakata H, Yoshimine Y, Maruyama E, Terakawa A, Tanaka M and Kiyama S 2005 *Proc. 31st IEEE Photovoltaic Specialist Conf. (Lake Buena Vista, FL)* (New York: IEEE) pp 866–71
- [3] Zhao J, Wang A, Green M A and Ferraza F 1998 *Appl. Phys. Lett.* **73** 1991
- [4] Blakers A W, Wang A, Milne A M, Zhao J and Green M A 1989 *Appl. Phys. Lett.* **55** 1363
- [5] Kerr M J, Cuevas A and Campbell P 2003 *Prog. Photovolt.* **11** 97
- [6] Swanson R M 2005 *Proc. 20th Eur. Photovoltaic Solar Energy Conf. (Barcelona, Spain)* (Munich: WIP-Renewable Energies) pp 584–9
- [7] King R R, Sinton R A and Swanson R M 1990 *IEEE Trans. Electron Dev.* **37** 365
- [8] Cuevas A, Basore P A, Giroult-Matlakowski G and Dubois C 1996 *J. Appl. Phys.* **80** 3370
- [9] Kerr M J, Schmidt J, Cuevas A and Bultman J H 2001 *J. Appl. Phys.* **89** 3821
- [10] Sinton R A and Cuevas A 1996 *Appl. Phys. Lett.* **69** 2510
- [11] Cuevas A and McDonald D 2004 *Sol. Energy* **76** 255
- [12] Clugston D and Basore P 1997 *Proc. 26th IEEE Photovoltaic Specialists Conf. (Anaheim)* (New York: IEEE) pp 207–10
- [13] Martin I, Vetter M, Orpella A, Puigdollers J, Voz C, Alcubilla R, Lacoste J D and Roca P 2004 *Proc. 19th Eur. Photovoltaic Solar Energy Conf. (Paris, France)* (Munich: WIP-Renewable Energies) pp 2194–7
- [14] Cousins P J, Neuhaus D H and Cotter J E 2004 *J. Appl. Phys.* **95** 1854
- [15] Nijs J F, Szlufcik J, Poortmans J, Sivonthaman S and Mertens R P 1999 *IEEE Trans. Electron Dev.* **46** 1948
- [16] Hilali M M, Nakayashiki K, Ebong A and Rohatgi A 2006 *Prog. Photovolt.* **14** 135
- [17] Kerr M J and Cuevas A 2002 *Semicond. Sci. Technol.* **17** 35
- [18] Cuevas A and Sinton R A 1997 *Prog. Photovolt.* **5** 79